Available online at www.sciencedirect.com

ScienceDirect

Procedia Structural Integrity 19 (2019) 719–728

Structural Integrity Procedia

www.elsevier.com/locate/procedia

Fatigue Design 2019

Fatigue behaviour of gear teeth made of case hardened steel: from competing mechanisms to lifetime variability

Vincent ARGOUD[a,b], Franck MOREL[a,*], Etienne PESSARD[a], Daniel BELLETT[a], Simon THIBAULT[b], Stéphane GOURDIN[b]

[a]*LAMPA, Arts et Métiers ParisTech Angers, 2 Bd du Ronceray, 49035 Angers, France*
[b]*Safran Tech, Materials and Processes Department, Rue des Jeunes Bois, Châteaufort, 78114 Magny-Les-Hameaux, France*

Abstract

Jet engines gears are generally made of steel and are case-strengthened via thermochemical treatments such as carburizing or nitriding causing microstructural modifications, superficial hardening and compressive residual stresses in the surface layers. These treatments increase the resistance to cyclic loads caused by contact between teeth and by the bending loads applied to the teeth. These two loading modes create high stress gradients at the surface. A large number of studies concerning the effect of thermochemical treatments on fatigue resistance have been carried out for uniaxial loads (rotating bending, tension or plane bending). Most of them were undertaken using smooth specimens, which do not correctly reproduce the stress gradient at the root of the gear teeth. A strong dependence between the loading mode and the position of the crack initiation site is also observed. The present work aims at experimentally investigating the fatigue behaviour of case hardened steel with a special focus on crack initiation and growth mechanisms. A vast experimental campaign composed of two parts is undertaken. Firstly, a Single Tooth Bending Fatigue (STBF) test is carried out on gears made of 16NiCrMo13 carburized steel. The resulting Wöhler diagram shows high scatter at certain stress levels which suggests a bi-modal behaviour, characterized by very different crack initiation kinetics. Secondly, fatigue tests conducted on notched specimens loaded in plane bending, designed to accurately reproduce the stress gradient observed at the gear tooth root are carried out to confirm this bimodal behaviour and to characterize the failure mechanisms.

Peer-review under responsibility of the Fatigue Design 2019 Organizers.

Keywords: Fatigue ; HCF ; Gear ; Steel ; Thermochemical treatment ; Case hardening ; Statistical behaviour

1. Introduction

Gears are used by the aerospace industry in different systems such as jet engine and helicopter gearboxes. These parts, generally made of steel, can have rotational velocities of up to tens of thousands of rotations per minute while being loaded several times per rotation. Therefore, their fatigue strength plays a major role in their design. Via the analysis of more than 1500 studies, Becker *et al.* (2002) report that tooth root bending fatigue is one of the three most

* Corresponding author. Tel.: +0-000-000-0000 ; fax: +0-000-000-0000.
E-mail address: franck.morel@ensam.eu

2452-3216
Peer-review under responsibility of the Fatigue Design 2019 Organizers.
10.1016/j.prostr.2019.12.078

common failure modes in gears (in addition to tooth bending impact and abrasive tooth wear). In all cases (contact and bending), the stress is concentrated close to the surface. Consequently, thermochemical treatments such as carburizing or nitriding are common solutions to enhance the fatigue resistance of gears by increasing the surface hardness and adding compressive residual stress at the surface. The current need to radically reduce transportation costs while maintaining the level of security requires both reliable and precise knowledge of the impact of such thermochemical treatment on the fatigue behaviour of low alloyed steel.

Many studies, both on gears and specimens, concerning the fatigue behaviour of case hardened or nitrided steel are available. Single Tooth Bending Fatigue (STBF) tests on gears are usually considered as being the most reliable but the testing conditions are complicated to master and those tests are expensive. The use of specimens has several advantages such as the lower cost or the higher testing frequency and it is generally easier to use measurement equipment. However, studies carried out on specimens often show a lack of representativeness. The specimen geometry is typically the root cause of this problem. If the geometry is not chosen correctly it leads to a significant different applied stress field and subsequently to different fatigue behaviour. For instance, the fact that the fatigue resistance is greater with the increase of the Case Hardening Depth (CHD, depth below the surface where the hardness decreased to 550 HV) is shown by Genel *et al.* (1999) for carburized AISI 8620 steel and by Barrallier *et al.* (1994) on nitrided 33CrMoV12 steel, both for smooth cylindrical specimens in rotating bending. On the other hand, Tobie *et al.* (2017) showed thanks to STBF tests that while the fatigue resistance as a function of the CHD initially increase, it reaches a maximum before slightly decreasing. The testing conditions (*i.e.* loading mode and specimen geometry) also have an influence on the crack initiation position (Thibault, 2019). During STBF tests, tooth root cracks almost always initiate at the surface or at a depth less than 100 µm but always in the carburized/nitrided layer (Gasparini *et al.*, 2008), (Shen *et al.*, 2011), (Gorla *et al.*, 2017). Concerning tests on specimens, the crack initiation position changes depending on the geometry. For smooth cylindrical specimens in rotating bending (Genel *et al.*, 1999) or tension-compression (Limodin *et al.*, 2006), crack initiation mainly occurs at the case-core interface with a lower fatigue strength. For cylindrical notched specimen, the crack tends to initiate at the surface if the surface stress gradient χ is high enough and at the case-core interface for a blunt notch.

In conclusion, the literature review highlights the fact that the majority of specimen data available is not representative of the real application and the STBF tests for other materials do not give enough information concerning the fatigue mechanisms. Hence, further experimental work is needed. Considering the effect of the specimen geometry on the fatigue behaviour, it is proposed that a notched specimen with a rectangular section, loaded in plane bending be used to precisely reproduce the loading mode at the gear teeth root.

This study is focussed on the High Cycle Fatigue (HCF) behaviour of the carburized low alloyed 16NiCrMo13 steel used for manufacturing gears for the aeronautical industry. It aims at proposing, for a given gear geometry, a method to design a notched plane bending specimen that is representative of the tooth root. Both STBF tests on gears and plane bending fatigue tests on specimens are carried out in order 1) to evaluate the representativeness of the notched specimens, 2) to evaluate the fatigue strength of the carburized 16NiCrMo13 steel and 3) to analyse the crack initiation mechanism(s) thanks to a fractographic analysis in order to correlate it with the fatigue response.

2. Experimental conditions

2.1. Material and thermochemical treatment

The studied material is a low-alloy 16NiCrMo13 steel whose yield stress is about 1050 MPa and ultimate stress is about 1350 MPa. The chemical composition is given in table 1.

Once machined, the parts are austenitized then low-pressure carburized in an environment of sufficient carbon potential to cause absorption of carbon at the surface and, by diffusion, create a carbon concentration gradient between the surface and the core (fig 1). The parts are then quenched to obtain a martensitic structure wich allows the surface to reach 710 to 730 HV while the core remains at 420 HV (fig. 2). A cryogenic treatment is finally applied to limit residual austenite, followed by a stress relieve treatment. The martensitic transformation occurs initially at the limit of the case producing strain incompatibilities and compressive residual stresses (fig. 3), that are considered beneficial for the bending fatigue life.

Table 1: Chemical composition (wt %) of 16NiCrMo13 steel.

	Fe	C	Mn	Si	Cr	Ni	Cu	Mo	P	S
Minimum	Base	0.13	0.30	0.15	0.80	3.00	-	0.20	-	-
Maximum	Base	0.17	0.60	0.40	1.10	3.50	0.35	0.30	0.015	0.010

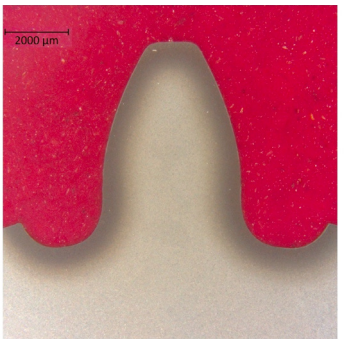

Fig. 1: Micrographie of a tooth of a carburized gear (etched with a 4% nital solution)

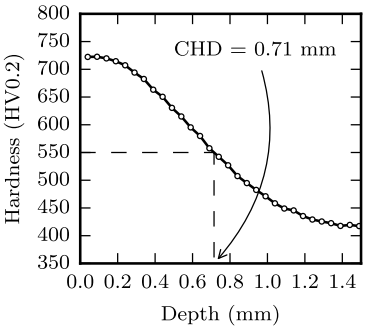

Fig. 2: Hardness profil.

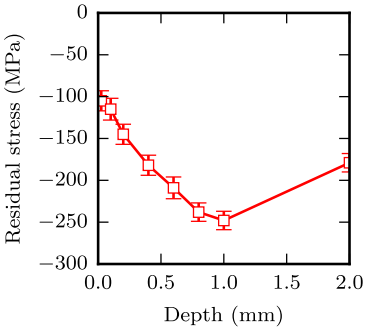

Fig. 3: Residual stress profil.

2.2. *Specimens*

The two specimen types investigated, gears specimens and notched specimens, are shown in fig 4a. The gear specimens are machined from a 16NiCrMo13 forged bars and then carburized before grinding of the flank surfaces (note that the tooth root surface condition remains as machined). The principal geometric characteristics of the gear specimens are listed in table 2. Six teeth evenly distributed around the circumference are removed from each gear in order to adapt it to the test bench (fig 5) and the number of teeth remaining provides the possibility to perform 5 fatigue tests per gear.

Table 2: Main characteristics of tests gears specimens.

Characteristic	**Symbol**	**Unit**	**Value**
Module	m	mm	2.54
Number of teeth	z	-	24
Face width	b	mm	10
Pressure angle	α	deg	20
Helix angle	β	deg	0
Root fillet	ρ_F	mm	from 1.11 to 1.45
HPSTC	-	mm	28.58

The notched specimens are designed in order to accurately reproduce the stress conditions at the tooth root of the gear specimen. To do so, several methods were tested by Argoud *et al.* (2017) and the most accurate remains to duplicate the mains geometric characteristics of the tooth (see fig. 4b). Mechanical finite element simulations were made for both the gear and the specimen designed with this method. The three normalized principals stress components and the normalized von Mises stress (σ_e) are shown as a function of the depth in fig. 4c for the root of the gear used in this study and its corresponding notched specimen. The path used to draw the stress distributions starts

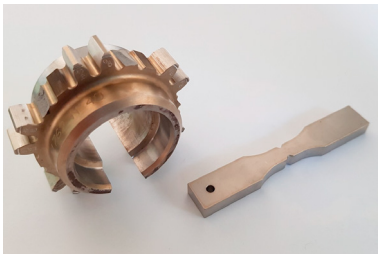

(a) Picture of a tested gear specimen and a notched specimen.

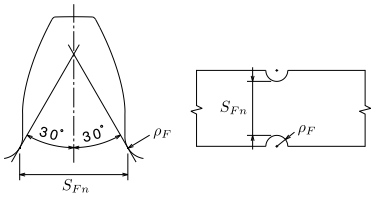

(b) Sketch of a gear tooth and the corresponding notched specimen.

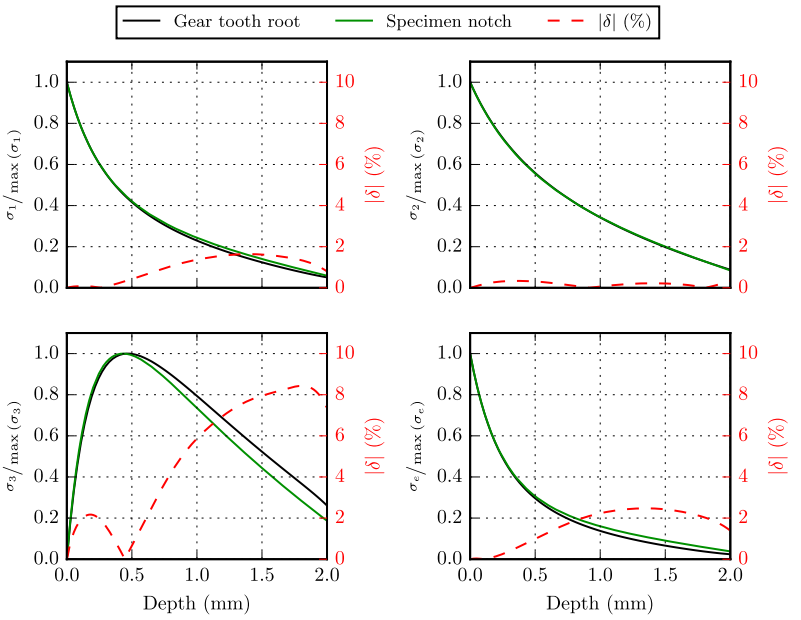

(c) Normalized principals stresses (σ_1, σ_2 and σ_3) and the normalised von Mises equivalent stress (σ_e), at the gear tooth root and at the specimen notch via elastic finite element analyses.

Fig. 4: Gears and notched specimens characteristics.

at the stress hot-spot and goes into the material in the direction normal to the surface at the hot-spot. The absolute relative error $|\delta|$ is also calculated in order to show the correlation between the stress fields of the two structures.

As it is impossible to accurately reproduce the tooth root surface conditions at the specimen notch, it was decided to grind the notch in order to obtain a 0.4 µm arithmetical mean height roughness (Ra). In order to be compatible with the maximum loads of the testing machines, the width of the bending specimen is 6 mm while the tooth face width is 10 mm. Finally, in order to obtain the same metallurgical properties, the notched specimens are made of the same 16NiCrMo13 steel bar as the gear specimens and the carburization parameters are also the same.

2.3. Testing equipment

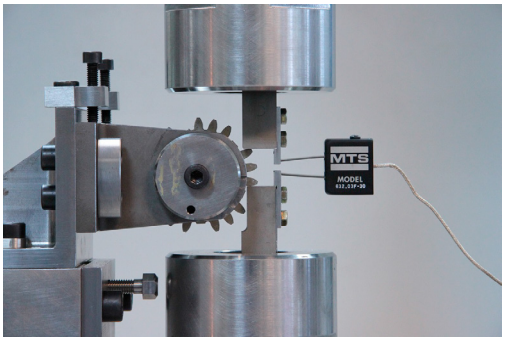

Fig. 5: Gear specimen mounted in the STBF bench.

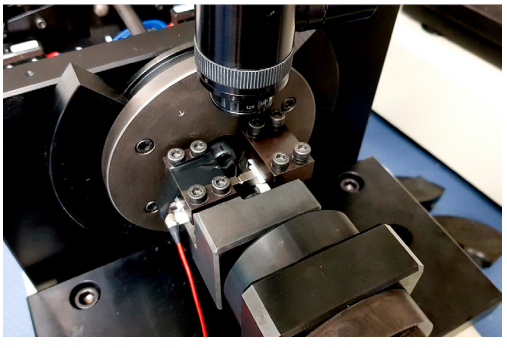

Fig. 6: Plane bending bench.

Two testing benches are used in this study. The first is a Single Tooth Bending Fatigue (STBF - fig. 5) test bench that was specifically designed to be used on a standard MTS 100 kN servo-hydraulic fatigue testing machine. In this experimental set-up the gear is held via its axis and is free to rotate about this axis. All other possible movements are

blocked. However, its vertical position can be precisely adjusted in order to control the location of the contact between the teeth and the anvils. The two contact anvils are made from carburized 16NiCrMo13 steel and are ground in order to obtain a very hard and smooth plane contact surface to limit wear and friction. One of the two anvils is fixed and is used to block the rotation of the gear, the other anvil moves with the hydraulic actuator of the fatigue machine and is used to load the gear. This kind of set-up implies that two teeth must be loaded during each test. However, because the force $\mathcal{F}$ is apply closer to the tip for one tooth and closer to the root for the other, only one of the two loaded teeth is actually being tested. The first principal stress at the tooth root σ_1 for a given applied force at the HPSTC[1] is usually estimated thanks to the international standard ISO 6336-3 (2006). In order to increase the stress level difference between the two loaded teeth, the load is applied 1 mm higher than the HPSTC. The stress at the root is estimated thanks to a finite element analysis done using Abaqus. The author (Argoud *et al.*, 2017) shows that the stress hot-spot position at the root remains unmodified with the loading position change. Different load cases have been tested on the bench and then simulated with Abaqus. The comparison of the results made it possible to estimate the friction coefficient between the tooth flank and the anvils, which has an important influence on the stress at the root. Furthermore, as the root radius ρ_F can significantly change from one tooth to another, it appears in the relation between σ_1 and $\mathcal{F}$ in order to reduce the variability caused by geometrical changes. During the test, a sinusoidal load is applied at a frequency of 40 Hz with a constant load ratio $R = 0.05$. The displacement d of the movable anvil is measured with an extensometer during the test. Each test ended if a tooth did not fail before 10^7 cycles or if the variation of d_a, the amplitude of d, was greater than 0.02 mm (fig. 7).

The second test bench is used to perform plane bending fatigue tests and consists of a RUMUL Cracktronic resonant testing machine (fig. 6) which can apply a maximum bending moment of 160 Nm. Both 0.05 and -1 load ratio can be used by ajusting the mean and amplitude bending moment. With this machine, as the specimen stiffness decreases when a crack grows, crack initiation can be detected via a drop in the natural frequency (Δf) of the system. In this study, the frequency drop is set to 0.5 Hz (fig. 8). This testing machine is easy to use and more convenient, especially when tests need to be stopped and re-started, for instance in order to make silicone rubber replications of the notch to measure the crack growth.

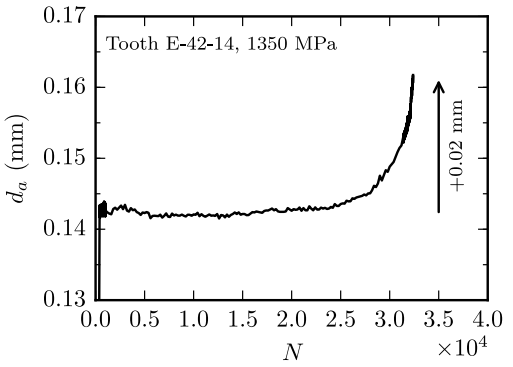

Fig. 7: Crack initiation criterion for a gear specimen.

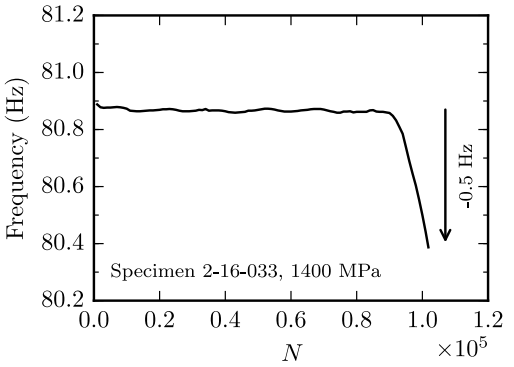

Fig. 8: Crack initiation criterion for a notched specimen.

3. Fatigue tests results

3.1. STBF

In total, 28 teeth have been tested. The first tooth was tested using the step-test method in order to obtain an estimation of the fatigue resistance which was then used as the stress level for the first test of the staircase procedure (Dixon *et al.*, 1948). For the first tooth, the initial stress level, σ_{max} (*i.e.* the value of maximum stress at the tooth root) was chosen to be 800 MPa. The stress was increased in steps of 50 MPa if no failure occurred after 10^6 cycles. On this

[1] The Highest Point of Single-Tooth Contact is the highest contact point on the teeth at which only one pair of tooth are in contact.

first tooth, a crack initiated at 1450 MPa after 109 226 cycles. As the stress level was surprisingly high, it was decided to start the staircase procedure at 1250 MPa. Thirteen teeth were used to estimate the fatigue resistance at 10^7 cycles. The staircase results in a median value of the fatigue limit of $\sigma_D = 1358$ MPa and the sample standard deviation of $s = 74$ MPa.

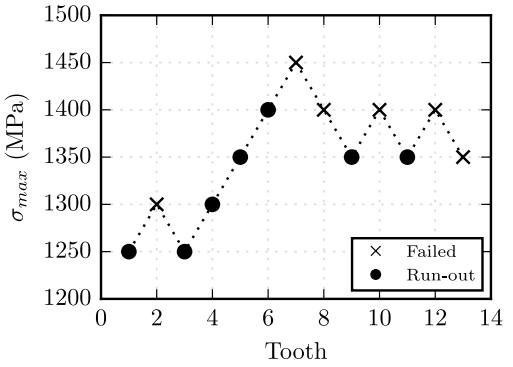

Fig. 9: Staircase sequence on gear specimens.

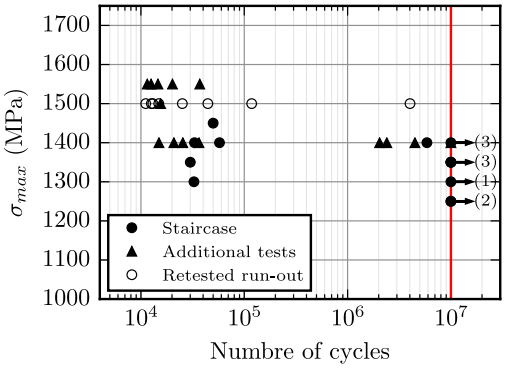

Fig. 10: Wöhler diagram of the gear specimens.

Among the fourteen remaining teeth, eight have been tested at 1400 MPa, five at 1550 MPa and the last one at 1500 MPa with the objective to give a better idea of the fatigue behaviour of the material. Finally, all the run-out teeth were retested at 1500 MPa to initiate a crack for further fractographic analysis. All the results are shown in fig. 10 in a Wöhler diagram. From this figure it can clearly be seen that the tests form two distinct groups: the first group contains specimens with a low number of cycles to failure (typically less than 10^5 cycles) and the second includes the specimens with a high number of cycles to failure (typically greater than 10^6 cycles) and the run-outs.

3.2. Plane bending on notched specimens

Carburized notched specimens have been tested with two main objectives: 1) to validate that they are representative of the gear tooth fatigue behaviour and 2) to investigate more precisely and more easily the fatigue behaviour of the carburized 16NiCrMo13 steel. The first specimen was tested using the step-test method (starting at 800 MPa with 50 MPa steps). A crack initiated after 791 274 cycles at the 1500 MPa stress level. Several tests were then performed at 1100, 1200, 1400 and 1600 MPa in order to give a general idea of the fatigue behaviour of the notched specimens. The plane bending results are shown in fig. 11 in addition to the STBF test results.

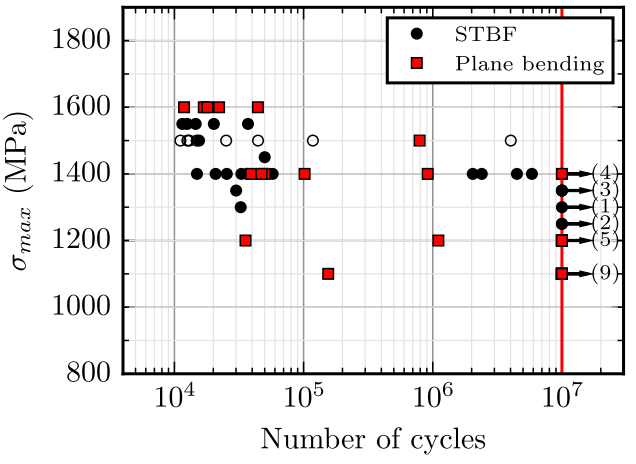

Fig. 11: STBF and plane bending fatigue results on a Wöhler diagram.

3.3. Fractographic analysis

For the STBF test, as the teeth were not totally broken, liquid nitrogen is used to induce the brittle failure of the cracked tooth. Using this method the fatigue crack propagation zones and the brittle failure zones are easier to distinguish on the failure surface. Visual observation makes it possible to note that the crack front (see fig. 12) is frequently slightly inclined, which suggests that crack initiation occurs preferentially close to a corner of the failure surface. This tendency is also observed for the notched specimens (fig. 13).

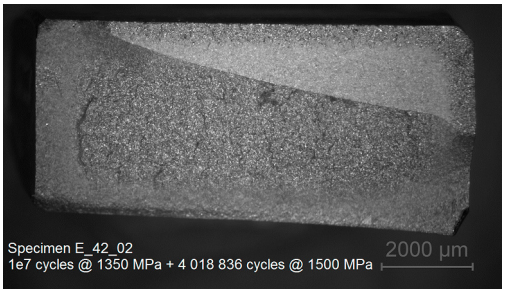

Fig. 12: Gear tooth fracture surface (d_a = 0.02 mm).

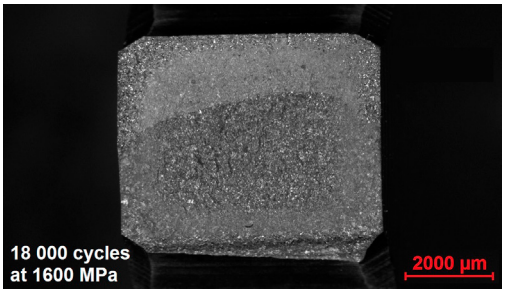

Fig. 13: Specimen fracture surface (Δf = 4 Hz).

The fractographic analysis is then carried out with a Scanning Electron Microscope (SEM). The fracture surfaces of the teeth show a prevailing intergranular crack propagation mode in the case hardened area (fig. 14a), which is typical of a brittle material. For the notched specimens, the interganular mode is less prevalent but still present (fig. 14b). The intergranular crack propagation gradually transforms into an transgranular propagation mode as the depth increases because of the hardness decrease. A closer analysis shows that, for both short and long lifetime, cracks initiate at the surface (fig. 14c, 14e and 14f), close to the specimen corners and at grain boundaries, forming an intergranular zone with the size of a few grains. Crack propagation then becomes transgranular for several tens of micrometers before becoming intergranular again. For one tooth, the crack initiated at a grain boundary about 30 µm below the surface and forms a fish eye (fig. 14d).

4. Discussion

The aim of this paper is to study the fatigue behaviour and crack initiation mechanisms of a gear specimen and a notched specimen, both made of carburized low alloyed 16NiCrMo13 steel. Specifically, a method has been proposed to define the geometry of a notched specimen so that it is representative of the fatigue behaviour of a given gear tooth root. The proposed method simply uses two key parameters of the gear teeth (the tooth root fillet ρ_F and the critical section S_{Fn}) to design the notched specimens. Static finite element calculations show very good correlation between both stress fields. The σ_1 and σ_2 principal stress components both lead to a relative error $|\delta|$ of less than 2%, from the surface up to a depth of 2 mm. The impact of the more significant error in the σ_3 component (*i.e.* the lowest principal stress) is quite low when it is used to compute an equivalent stress such as von Mises stress. Considering the results of the fatigue tests, fig. 11 shows a strong correlation between gear specimens and notched specimens fatigue behaviour. These results confirm the representativeness of the notched specimens.

The other objective of the fatigue tests is to study the fatigue behaviour of the carburized 16NiCrMo13 steel. Apart from the value of the fatigue resistance σ_D estimated thanks to the staircase procedure, an important result of this work concerns the variability in the life of the specimens (fig. 11). For instance, at 1400 MPa the 13 specimens tested show two very distinct data sets spaced by a large gap. The first set includes specimens with a fatigue life less than 10^5 cycles and the second one includes specimens with a fatigue life greater than 10^6 cycles. Considering the high number of tests undertaken at this stress level, the assumption of an effect due to a lack of data is not retained by the authors.

This type of result for fatigue tests on carburized or nitrided steel can be observed in different testing configurations. For instance, on STBF tests on carburized shot peened gears made of Ferrium C61 steel (Shen *et al.*, 2011) and nitrided 33CrMoV12 gears (Gorla *et al.*, 2017), on plane bending tests with modified Brugger sample made of carburized

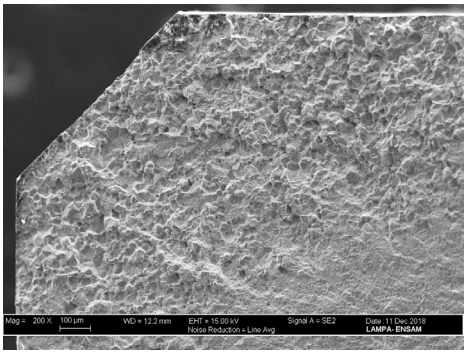

(a) Gear tooth fracture surface.

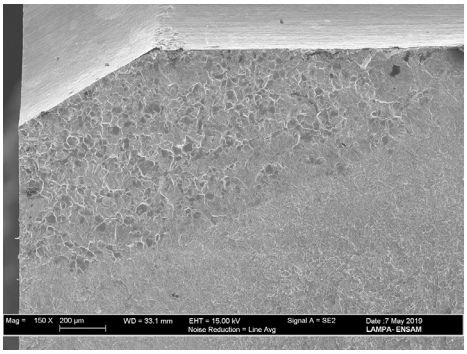

(b) Notched specimen fracture surface.

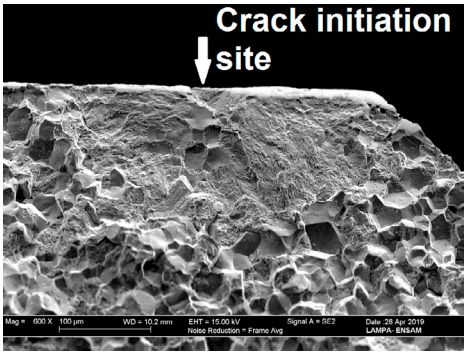

(c) Gear tooth crack initiation site (36 465 cycles at 1400 MPa).

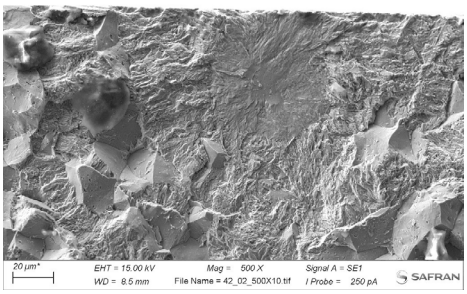

(d) Gear tooth crack initiation site (10^7 cycles at 1350 MPa + 4 018 836 cycles at 1500 MPa)

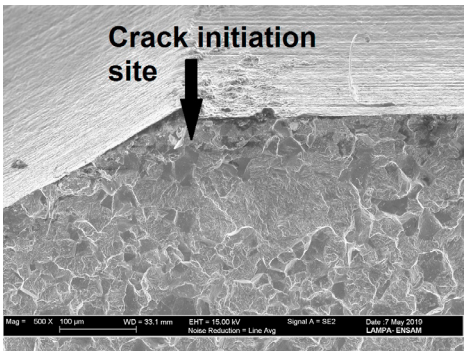

(e) Notched specimen crack initiation site (16 881 cycles at 1600 MPa).

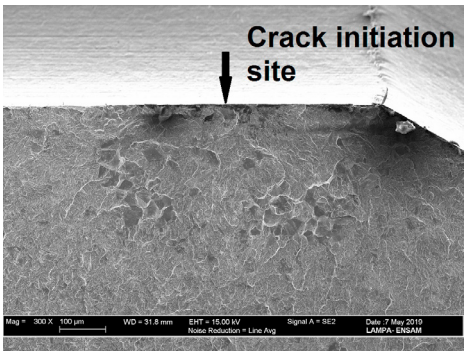

(f) Notched specimen crack initiation site (22 163 cycles at 1600 MPa).

Fig. 14: Fatigue failure surfaces of gear specimens and notched specimens.

SAE 4320 steel (Cohen *et al.*, 1991) and SAE 8620 steel (Spice *et al.*, 2002), on four points bending tests on smooth semi-cylindrical specimens made of carburized AISI 8620 steel (Apple *et al.*, 1973) or on axial tension-compression fatigue tests on notched cylindrical specimens made of gaz-nitrided AISI 4140 steel (Limodin *et al.*, 2006). However, in some other studies, this phenomenon is not observed. For instance, the Wöhler diagrams of the fatigue tests of Asi *et al.* (2009) (rotating bending on smooth cylindrical specimen, carburized SAE 8620 steel) and of Zhang *et al.* (2013) (STBF tests on carburized 20CrMoH gears) do not show any particular scatter. For now, among the different parameters (steel composition, thermochemical treatment, specimen geometry, sort of tests . . .), the authors are unable

to explain which one leads to this variability. Nevertheless, the data given by Apple *et al.* (1973) seem to show an increase in the gap with an increase in the surface hardness.

As far as we know, this specific phenomenon has never been highlighted in the case of carburized or nitrided steel. But in some situations, a large lifetime variability can be unequivocally explained by competing failure modes between surface and subsurface crack initiation, as shown by Chandran *et al.* (2010) in a beta-titanium alloy (Ti-10V-2Fe-3Al). In some cases, as shown by Jha *et al.* (2009) with the Ti6246, the lifetime variability is governed by the combination of a crack growth controlled life-limiting mechanism and a crack initiation controlled lifetime. The authors also show that if all experimental results are assumed to be due to a single crack initiation mechanism then the uncertainty would be increased while it could be reduced by using lifetime prediction based on the worst-case mechanism. More generally, Fischer *et al.* (2001), when studying electromigration failure distribution, show that the existence of two distinct failure mechanisms lead to a step-like shape of the cumulative density function (CDF).

Considering that the distribution of the failed tests at 1400 MPa can be described thanks to a Weibull distribution, let P_f, the cumulative probability that the specimen fails for a number a cycles N_f less than or equal to a given lifetime N. For a clearer representation, the Weibull sigmoïde is linearized by plotting $\ln\left(\ln\left(\frac{1}{1-P_f}\right)\right)$ over $\ln(N_f)$ on fig. 15. On the basis of this plot, it becomes obvious that data cannot be well described with only one CDF. The lifetime variability of the carburized 16NiCrMo13 seems thus to be driven by a bimodal failure mechanism. As the fractographic analysis of this present study does not highlight cracks at the case-core interface, another kind of failure mechanism duality must be acting. Unfortunately, the comparison of low and long lifetime specimens does not yet allow us to understand the two failures mechanisms.

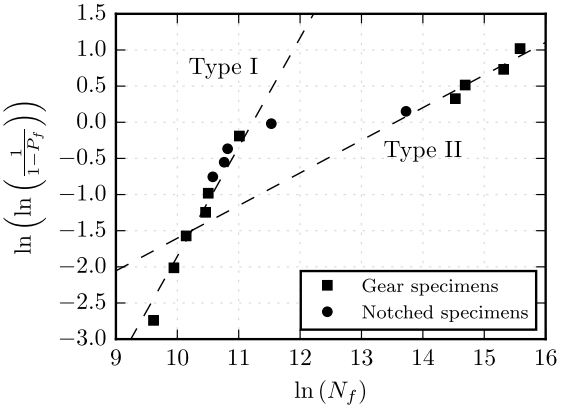

Fig. 15: Fatigue tests results at 1400 MPa in a linearized Weibull space.

Finally, it can be also be noticed that a crack has initiated at 1100 MPa and at 1200 MPa for the notched specimens (fig. 11). Due to the strong probability of specimens having a low life at stresses between 1300 and 1400 MPa, the staircase procedure does not allow to test relatively low stress levels (*i.e.* under 1300 MPa) thus additional tests must be conducted in order to get a better understanding of the fatigue strength. This information leads us to believe that the staircase method is not a suitable procedure to study the fatigue behaviour of this kind of material, with a large variability in lifetime and in stress.

5. Conclusion

Based on the current work concerning the fatigue behaviour of the carburized 16NiCrMo13 steel, the following conclusions can be drawn:

1. the proposed method to design notched specimens is satisfactory to substitute STBF tests by plane bending tests;
2. the observed bimodal fatigue behaviour of the carburized 16NiCrMo13 steel is most probably due to a competition between two failure mechanisms, wich remains unidentified for now;

3. when a bimodal fatigue behaviour is detected, the staircase procedure may not be suitable and should at the very least be completed by additional tests.

Future work will focus on the comprehension of the two different failure mechanisms. Different measurements techniques will be used in future tests, such as acoustic emission or silicone rubber replications of the notch to improve the detection of the crack initiation and to measure the crack growth.

Acknowledgements

The author thanks Safran Tech (Saclay - France) for financial support, Safran Transmission Systems (Colombes - France) for realizing the carburizing treatments, Safran Aircraft Engines (Villaroche - France) for the design of the STBF test bench and for undertaking the fatigue tests on the gears. The author also thanks Myriam BROCHU from Polytechnique Montréal for his contribution to the fractographic analysis. Vincent Maurel and Alain Köster (Centre des Matériaux - Évry - France) are thanked for their contribution to the development of the STBF bench and the testing method.

References

AFNOR. NF ISO 6336-3 — Calcul de la capacité de charge des engrenages cylindriques à dentures droites et hélicoïdales — Partie 3 : Calcul de la résistance à la flexion en pied de dent. Association Française de Normalisation (AFNOR), Oct. 2006.

Apple, C. A., & Krauss, G. (1973). Microcracking and fatigue in a carburized steel. Metallurgical Transactions, 4(5), 1195-1200.

Asi, O., Can, A. C., Pineault, J., & Belassel, M. (2009). The effect of high temperature gas carburizing on bending fatigue strength of SAE 8620 steel. Materials & Design, 30(5), 1792-1797.

Argoud V., Maurel V., Köster A. & Thibault S. (2017). Développement doutils expérimentaux et numériques en vue de la prédiction de limite de fatigue de matériaux à gradient de propriétés, cas des dentures dengrenages renforcées par traitements thermochimiques. Master's thesis, MINES ParisTech - PSL Research University - Centre des Matériaux.

Barrallier L. (1994). Caractéristiques mécaniques des couches nitrurées. Cas des pièces en acier. Revue Traitement Thermique.

Becker, W. T., Shipley, R. J., Lampman, S. R.,*et al.* (2002). ASM handbook. Failure analysis and prevention, 11, 1072.

Chandran, K. R., Chang, P., & Cashman, G. T. (2010). Competing failure modes and complex SN curves in fatigue of structural materials. International Journal of Fatigue, 32(3), 482-491.

Cohen, R. E., Haagensen, P. J., Matlock, D. K., & Krauss, G. (1991). Assessment of bending fatigue limits for carburized steel (No. 910140). SAE Technical Paper.

Dixon, W. J., & Mood, A. M. (1948). A method for obtaining and analyzing sensitivity data. Journal of the American Statistical Association, 43(241), 109-126.

Fischer, A. H., Abel, A., Lepper, M., Zitzelsberger, A. E., & Von Glasow, A. (2001). Modeling bimodal electromigration failure distributions. Microelectronics Reliability, 41(3), 445-453.

Gasparini, G., Mariani, U., Gorla, C., Filippini, M., & Rosa, F. (2008). Bending fatigue tests of helicopter case carburized gears: Influence of material, design and manufacturing parameters. In American Gear Manufacturers Association (AGMA) Fall Technical Meeting (pp. 131-142).

Genel, K., & Demirkol, M. (1999). Effect of case depth on fatigue performance of AISI 8620 carburized steel. International Journal of Fatigue, 21(2), 207-212.

Gorla, C., Rosa, F., Conrado, E., & Concli, F. (2017). Bending fatigue strength of case carburized and nitrided gear steels for aeronautical applications.

Jha, S. K., Larsen, J. M., & Rosenberger, A. H. (2009). Towards a physics-based description of fatigue variability behavior in probabilistic life-prediction. Engineering Fracture Mechanics, 76(5), 681-694.

Limodin, N., & Verreman, Y. (2006). Fatigue strength improvement of a 4140 steel by gas nitriding: Influence of notch severity. Materials Science and Engineering: A, 435, 460-467.

Shen, T., Krantz, T., & Sebastian, J. (2011). Advanced Gear Alloys for Ultra High Strength Applications. NASA technical report 2011-217121.

Spice, J. J., Matlock, D. K., & Fett, G. (2002). Optimized carburized steel fatigue performance as assessed with gear and modified brugger fatigue tests. SAE Transactions, 589-597.

Thibault, S. (2019). Caractérisation mécanique des couples aciers/traitement thermochimiques pour transmission de puissance. Importance des types de sollicitation. Journée technique A3TS Fatigue et Corrosion.

Tobie, T., Hippenstiel, F., & Mohrbacher, H. (2017). Optimizing gear performance by alloy modification of carburizing steels. Metals, 7(10), 415.

Zhang, J., Zhang, Q., Xu, Z. Z., Shin, G. S., & Lyu, S. (2013). A study on the evaluation of bending fatigue strength for 20CrMoH gear. International Journal of Precision Engineering and Manufacturing, 14(8), 1339-1343.